JOURNAL OF MATERIALS SCIENCE 33 (1998) 3831–3837

Diffusion annealing of Fe–Ni alloy coatings on steel substrates

F. CZERWINSKI*
Department of Metallurgical Engineering, McGill University, Montreal, Canada H3A 2B2
E-mail: Frankcz@minmet.lan.mcgill.ca

A two-stage surface treatment of steel is described. During the first stage, a steel surface is coated with an Fe–14% Ni electrodeposit having an initial hardness of 300–400 HV. Subsequently, the microstructure and hardness of the coatings are modified by thermal and thermochemical treatment. The annealing at temperatures between 500 and 1000 °C leads to the diffusion of carbon from the substrate to the coating and an increase in coating hardness after cooling. In some cases, the enrichment of coating in carbon is enhanced by applying an external source of carbon and nitrogen. As an example, carburizing and carbonitriding in solid media are presented. Owing to a difference in the temperature of the α–γ phase transformation between the steel substrate and the Fe–Ni coating, the thermal treatment is conducted at a coexistence of α–γ or γ–γ diffusion couples. This allows us to obtain the various microstructure and depth-profiles of hardness across the coating thickness and the adjacent region of the substrate. Some benefits of the proposed surface treatment are discussed.

1. Introduction

The electrodeposited Fe–Ni alloy coatings have been exploited for many years to impart special surface properties to structural and engineering components. While alloys rich in nickel are known for superior magnetic properties [1], the alloys rich in iron have good wear resistance and corrosion resistance [2]. An additional advantage of Fe–Ni electrolytic alloys is the high rate of deposition, up to sixteen times greater than that achieved during growth of chromium, and a possibility to produce coatings with thicknesses up to 2 mm [3]. These factors make Fe–Ni alloys an excellent material to restore used or improved new surfaces of various elements.

In order to obtain a high wear resistance, very often exceeding the values typical for tempered steel, Fe–Ni alloys have to be deposited under a condition of high polarization. As a result, electrodeposits are under high internal stress, which is frequently the cause of microcracks [4, 5]. Tensile stress, typical for Fe–Ni alloys, and microcracks limit the exploitation of the coatings: they may cause localized corrosion and a decrease in fatigue life of the coated part, in some cases up to 40% [6]. Therefore, to obtain a good combination of corrosion and wear resistance and in order not to deteriorate the fatigue life of the coated element, the electrolytic coating should have a high hardness, be compact (microcrack free) and exhibit low tensile stress.

In order to manufacture coatings having the above behaviour, a two-stage surface treatment is proposed. At first, the compact coating of Fe–Ni alloy is deposited on the steel substrate and then the coating is subjected to heat treatment. The objective of this study was to verify the possibility of modifying the microstructure and hardness of Fe–Ni electrolytic coatings deposited on a steel substrate by applying diffusion annealing.

2. Experimental procedure

Fe–Ni alloy coatings with thicknesses up to 350 μm were deposited from an electrolyte composed of nickel chloride and ferrous chloride with concentrations of 200 and 300 g dm^{-3}, respectively. pH was kept constant at a level of 1.5 by the addition of hydrochloric acid. Deposition was conducted galvanostatically at a current density of 250 mA cm^{-2} and the electrolyte temperature of 85 °C. Pure iron was used as an anode. As substrates for coating deposition, steel containing 0.91% C and iron, were used. Chemical compositions of substrates and anodes are given in Table I.

Substrate surfaces were prepared by mechanical polishing up to 800-grit SiC paper, followed by chemical polishing in 10% hydrochloric acid. Diffusion annealing was conducted in the tube furnace in a flowing argon atmosphere. The specimens 10 mm × 10 mm × 5 mm in size were cooled from an annealing temperature in air or in water. The carburizing and carbonitriding processes were performed in solid media. For carburizing, the mixture containing 90% charcoal and 10% Na_2CO_3 was used. The carbonitriding was carried out in a mixture of KCN, KCNO, and K_2CO_3 with weight ratios of 45, 45, and 10,

*On leave from the University of Mining and Metallurgy, Coacow, Poland

TABLE I The chemical compositions (wt %) of substrates, anodes and coatings

Material	C	Si	Mn	P	S	Cr	Ni
Fe–Ni coatings	–	0.062	–	0.022	0.014	0.032	14
Steel substrates	0.91	0.20	0.28	0.014	0.015	0.040	0.06
Iron substrates and anodes	0.03	0.05	0.14	0.012	0.014	–	–

respectively. The microstructure on cross-sectional and planar specimens was examined using optical and transmission electron microscopy (TEM). Samples for optical microscopy were etched in a 3% solution of nitric acid in ethanol. Hardness measurements were performed on polished cross-sections at different distances from the substrate/deposit interface using a Vickers microhardness tester with a pyramid indentor. A load of 100 g was applied and the final value quoted for the hardness of a deposit is the average of at least five measurements. The standard deviations of these results were used to calculate the 95% confidence intervals that are placed on the graphs as error bars.

3. Results

3.1. Characterization of the coatings before annealing

The chemical composition of the coatings after deposition is shown in Table I. The average content of nickel was 14% and the impurities were kept at a very low level. There was evident cross-thickness segregation of the chemical composition: close to the substrate/coating interface, the nickel content was about 15% and decreased to about 11% at a thickness of 350 μm. Although it is difficult to express it quantitatively, there was also a detected increase in nickel content while moving from an interior towards the grain boundary of columnar crystallites. For that content of nickel, according to the equilibrium diagram [7], two phases, α and γ, should coexist (Fig. 1). Thus, the presence of a solely α phase after deposition indicates that the alloy is not in a state of equilibrium. Microstructural investigations revealed that coatings were composed of columnar grains with the column axis parallel to the growth direction and normal to the substrate surface. Many of the grains had a columnar length almost equal to the thickness of the coating. The diameter of the columnar grains, as measured on the plane parallel to the substrate surface, increased during deposit growth. For example, during the change of coating thickness from 35 μm to 90 μm the cross-sectional grain size increased from 1.3 μm to 2.6 μm [8]. Details of the coating microstructure after deposition are published previously [8].

3.2. Microhardness of the coatings after annealing

The microhardness of as-deposited coatings was about 420 HV in the region close to the substrate and

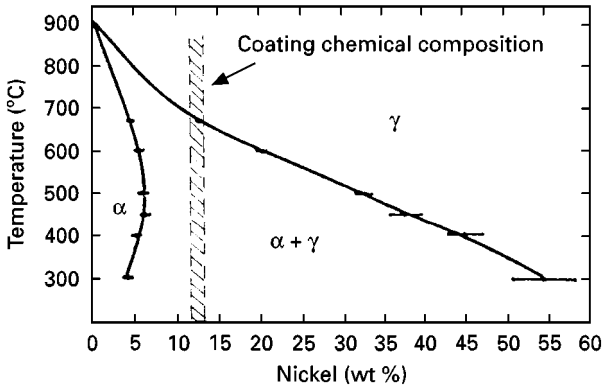

Figure 1 The iron-rich part of Fe–Ni equilibrium phase diagram [7]. The average chemical composition of coatings used in this study is indicated.

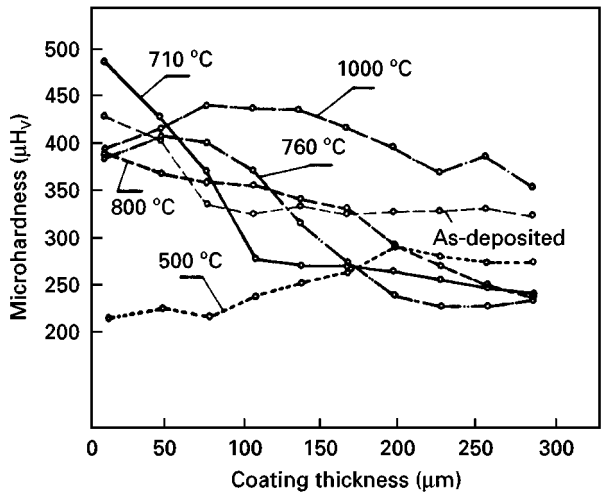

Figure 2 The influence of the annealing temperature on the microhardness of Fe–Ni coatings deposited on the steel substrate. The microhardness of the coating before annealing is indicated. For typical error bars, see Fig. 3. Diffusion annealing, time = 0.5 h, air-cooling.

decreased to about 320 HV at a thickness of 300 μm (Fig. 2). Annealing for 0.5 h at temperatures between 500 and 1000 °C followed by air-cooling, changed significantly the coating hardness. As shown in Fig. 2, annealing at 500 °C caused a reduction in coating hardness throughout the whole thickness of 300 μm. An especially low hardness of approximately 200 HV was observed in 100 μm thick region adjacent to the substrate. After annealing at 710 and 760 °C the hardness of the near substrate region was generally increased, but at the thicknesses beyond 100–150 μm it was still lower than that after deposition. Annealing at 800 °C caused a reduction in hardness in the 70 μm thick near-substrate region. The middle part of the coating was slightly harder than that after deposition and the region beyond 170 μm had a hardness similar to that after annealing at lower temperatures. A temperature of 1000 °C caused an increase in coating hardness throughout the whole thickness. Only a very thin layer adjacent to the substrate had a hardness lower than that after deposition.

In order to verify the influence of carbon present in the steel substrate on coating hardening after annealing, two kinds of substrates with essentially different carbon contents were used. As shown in Fig. 3, the annealing at 1000 °C followed by air cooling of the coating deposited on pure iron (0.03% C) led to a reduction in coating hardness to the level of 250 HV. At the same time, identical annealing of the coating deposited on the steel containing 0.91% carbon led to an increase in hardness, as presented above.

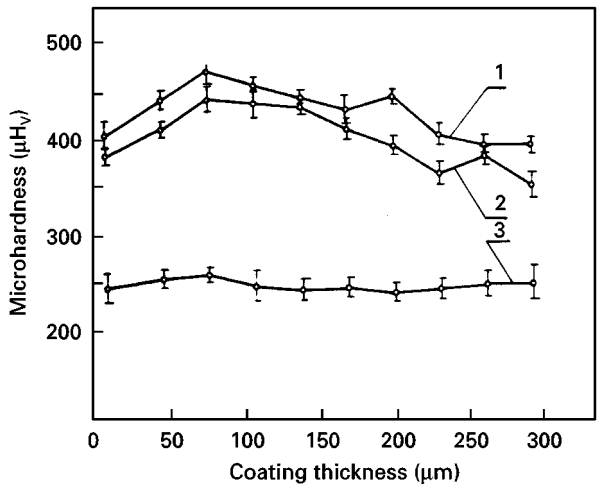

Figure 3 The influence of carbon content in the substrate, and the cooling rate after annealing on the microhardness of Fe–Ni coatings: 1, steel substrate, water cooling; 2, steel substrate, air-cooling; 3, armco substrate, air-cooling. Diffusion annealing, 1000 °C, 0.5 h.

Fig. 3 also contains an example of the influence of the cooling rate after annealing on the coating hardness. The accelerated cooling rate, achieved by using water, caused a slight increase in coating hardness by approximately 50 HV, as compared to the cooling in air. A small difference in hardness indicates that due to a high content of nickel, the hardenability of the coating is high enough to transform austenite into martensite under air-cooling.

3.3. Microstructure of the coating and the steel substrate after heat treatment

The changes in hardness after annealing were accompanied by variations in coating microstructure. The major process expected to be effective during annealing at 500 °C is a recrystallization of the highly stressed regions of the coating. While this process presumably took place in a coating part adjacent to the substrate, the regions close to the outer surface still exhibited features of microstructural and microchemical inhomogeneity, which are typical for as-deposited alloy (Fig. 4a). At 650 °C the coating was in the two-phase $\alpha + \gamma$ region. As is shown in the cross-sectional (Fig. 4b) and planar view (Fig. 4c), the cores of columnar crystals remained untransformed and are

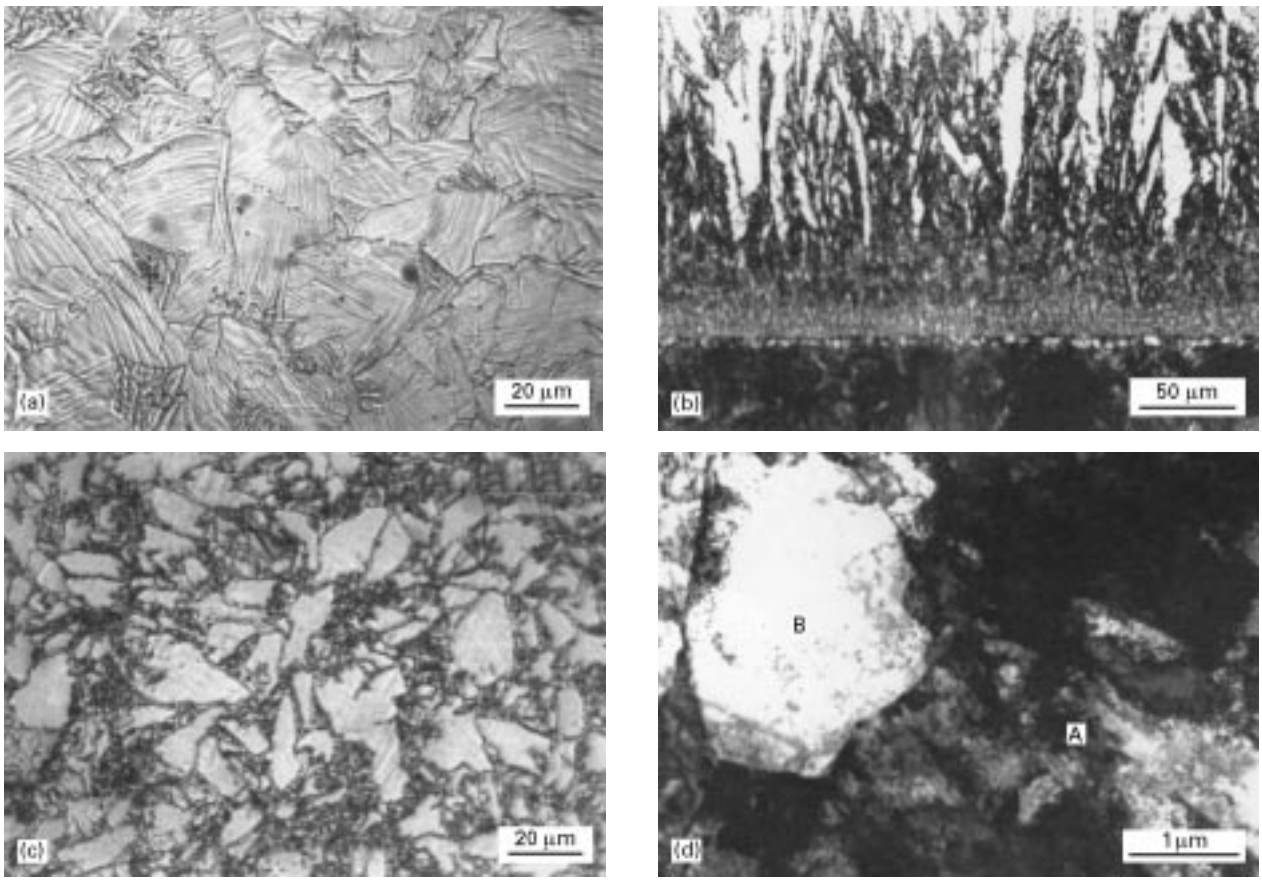

Figure 4 The microstructure of Fe–Ni coatings after diffusion annealing at temperatures below the α–γ phase transformation in the substrate. (a) 500 °C, 0.5 h, air cooling, planar section at a distance of 250 μm from the substrate/deposit interface; (b) 650 °C, 0.5 h, air-cooling, cross-sectional view; (c) planar-view of microstructure shown in (b) at a distance of 200 μm from the substrate/deposit interface; (d) TEM image of the microstructure shown in (c).

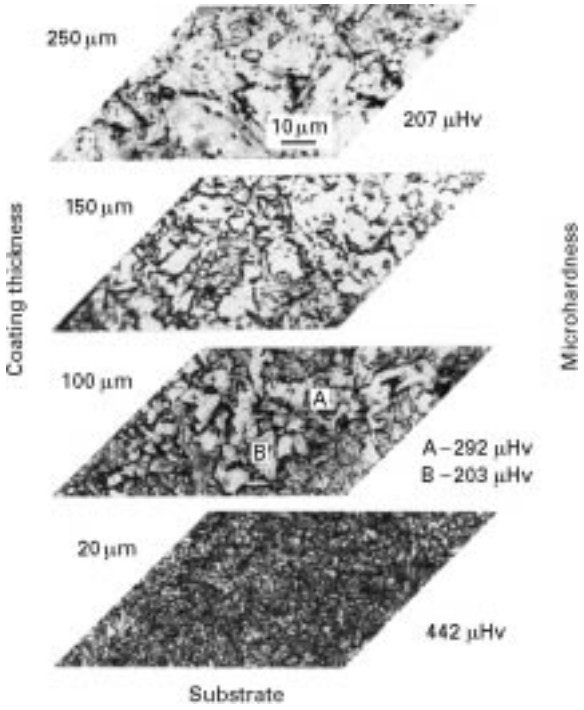

Figure 5 The microstructure of an Fe–Ni coating after diffusion annealing at 710 °C for 0.5 h followed by air-cooing. The distance from a substrate/deposit interface and the corresponding values of microhardness are indicated.

surrounded by fine-grained structures resulting from the decomposition of austenite. The ferrite which was not transformed to austenite at 650 °C is indicated as B in the transmission electron micrograph (Fig. 4d). The products formed after transformation of austenite during air-cooling, presumably a mixture of acicular ferrite and bainite, are marked A. The presence of these microstructural components caused an increase in coating hardness.

The microstructure of the coating after annealing at 710 °C, as imaged on planar sections at different distances from the substrate, is shown in Fig. 5. Ferrite which remained untransformed is marked B, while the products of austenite transformation are marked A. It is clear that with increasing distance from the substrate, the volume fraction of the transformed component is decreasing. Moreover, the microhardness of the austenite transformation products is decreasing in the same direction: at a distance of 20 μm it has a hardness of 442 HV, but at a distance of 100 μm its hardness dropped to 292 HV. Microstructurally, it corresponds to high carbon bainite in the near-substrate region and acicular ferrite close to the coating surface.

Heat treatment influenced not only the microstructure of the coating but also the microstructure of the substrate. During annealing at a temperature below the α–γ phase transformation of the steel (727 °C [9]),

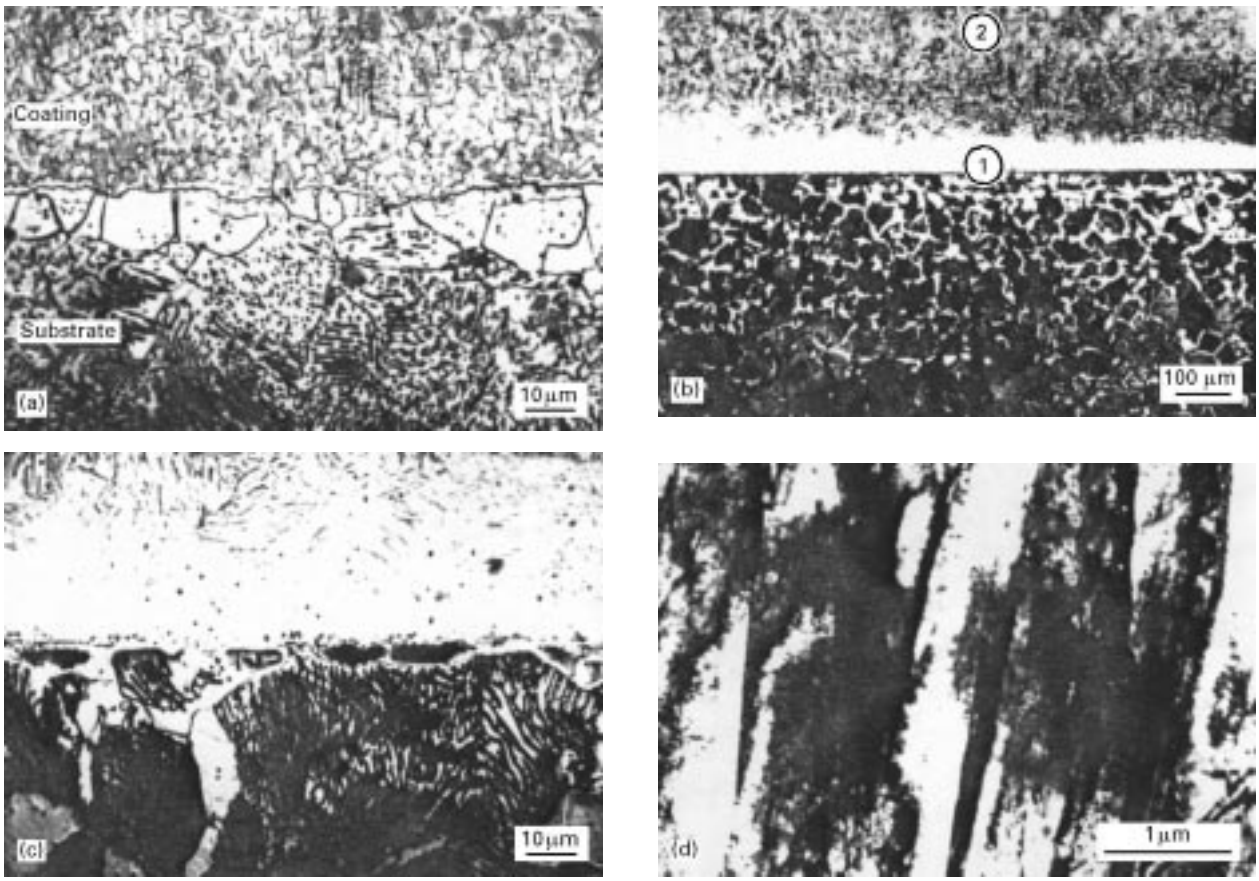

Figure 6 The influence of the annealing temperature in the range below and above the α–γ transformation for a steel substrate on the carbon redistribution and microstructure of the coating and adjacent regions of the substrate. (a) 710 °C, 0.5 h, air-cooling (cross-sectional view); (b) 1000 °C, 0.5 h, air-cooling (cross-sectional view); (c) region marked 1 in (b) (cross-sectional view); (d) TEM image of the region marked 2 in (b) (planar view).

the substrate microstructure was composed of 100% pearlite. Such a composition was deliberately selected to trace easily the diffusion of carbon on the basis of microstructural observations. A typical change is a decarburization of the substrate and the formation of a ferritic layer at the substrate/coating interface. For example, after 0.5 h annealing, the layer of ferrite had a thickness of approximately 10 μm (Fig. 6a).

Significantly different changes in coating microstructure were observed after annealing at temperatures higher than the α–γ transformation temperature of the steel substrate. Owing to a higher flux of carbon diffusing from the substrate, the coating exhibits after cooling, a microstructure composed of martensite and retained austenite (Fig. 6b and c). The detailed structure of martensite is shown in Fig. 6d. At temperatures above the 727 °C the substrate was austenitic and the diffusion of carbon to the coating took place as a result of the decarburization of austenite. Thus after cooling, the substrate did not show the ferritic layer, as described above, but ferritic and pearlitic microstructure with an increasing contribution of pearlite, while moving from the substrate/coating interface. After 0.5 h annealing at 1000 °C, the ferritic and pearlitic region is approximately 400 μm thick (Fig. 6b).

3.4. Microstructure and microhardness of the coatings after thermochemical treatment

The purpose of the thermo-chemical treatment is to provide the external source of carbon (carburizing) or simultaneously carbon and nitrogen (carbonitriding). It should be emphasized that at high temperatures the substrate also acts as a source of carbon and, in fact, during these processes the flux of the element causing hardening (C, N) is moving from two interfaces: the substrate/coating and gas/coating.

The changes in coating microhardness after carburizing are shown in Fig. 7. Because the coating is transformed to austenite at approximately 680 °C, carburizing can be also conducted at a temperature below the α–γ transformation temperature of the substrate. Such a treatment, performed at 710 °C, is represented by the lower curve in Fig. 7. An increase is seen in hardness in the regions adjacent to the substrate and to the outer surface, due to diffusion of carbon from these two directions. Carburizing at 920 °C allowed a higher enrichment of the coating in carbon and a higher hardness after cooling. It should be noted that a maximum hardness of the order 600–700 HV achieved after treatment at 920 °C is higher than that observed previously after annealing at 1000 °C. The lower hardness in the regions close to the substrate and the outer surface can be explained on the basis of

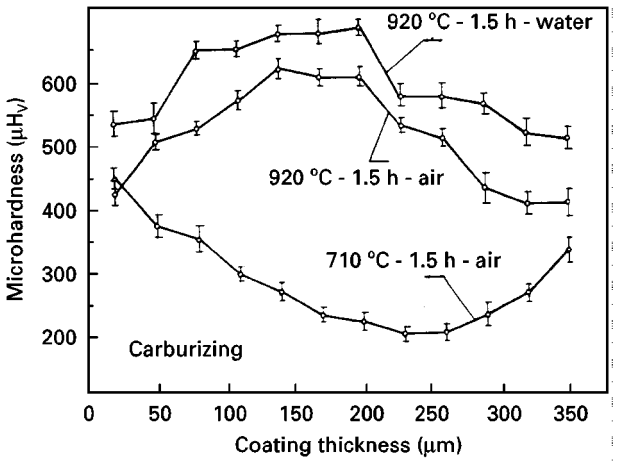

Figure 7 The effect of simultaneous diffusion annealing and carburizing on the microhardness of Fe–Ni coatings.

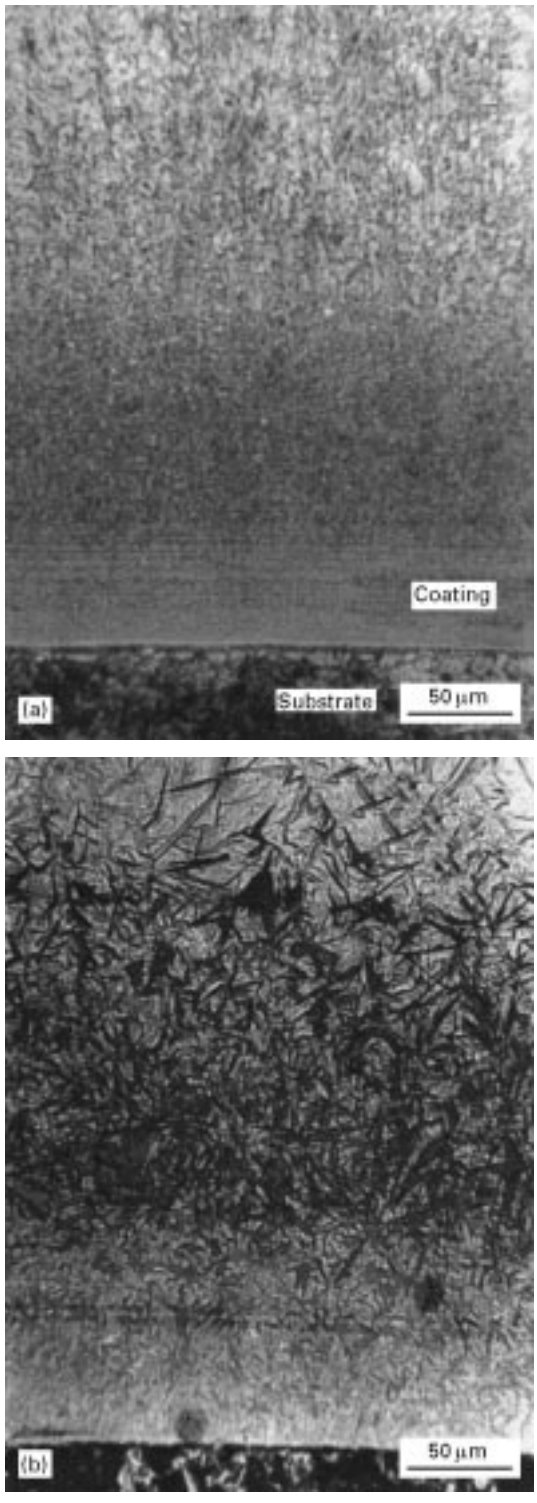

Figure 8 The microstructure of Fe–Ni coatings after simultaneous diffusion annealing and carburizing (a) 710 °C, 1.5 h, air-cooling; (b) 920 °C, 1.5 h, air-cooling.

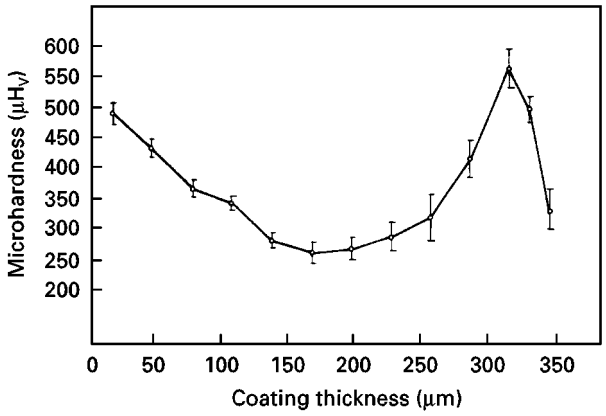

Figure 9 The effect of simultaneous diffusion annealing and carbonitriding on the microhardness profile across the coating thickness. KCN 45%, KCNO 45%, K_2CO_3 10%; 670 °C, 1.5 h, air-cooling.

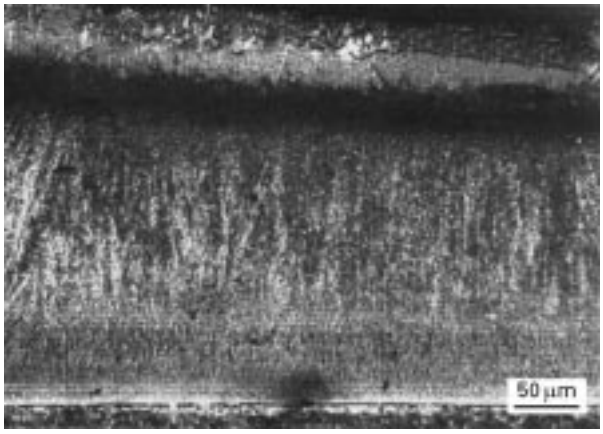

Figure 10 The effect of simultaneous diffusion annealing and carbonitriding on the coating microstructure (cross-sectional view).

microstructural observations. While the coating carburized at 710 °C has a microstructure of acicular ferrite and bainite (Fig. 8a), the coating carburized at 920 °C is composed of martensite and retained austenite (Fig. 8b). The high volume fraction of retained austenite in the regions close to the substrate and the outer surface caused the lower hardness, as observed in Fig. 7.

As a second example of thermo-chemical treatment, the carbonitriding in solid media is presented. The microhardness profile across the coating exhibits the maximum located in the sub-surface region (Fig. 9). A comparison with the corresponding microstructure (Fig. 10) indicates that it was caused by a layer of carbonitrides, typically situated in the near-surface region [10].

It should be emphasized that during carburizing and carbonitriding, the microstructural changes in the coating are accompanied by changes in the substrate. The extent of those changes is the same as that described previously for diffusion annealing.

4. Discussion

Electrolytic coatings are known to develop cross-thickness microstructural and microchemical inhomogeneity [11, 12]. For the coatings examined, this is expressed by changes of hardness as a function of a distance from the substrate (Fig. 2). At present, there is no clear explanation of the origin of inhomogeneities. It is possible that changes in current microdistribution caused by the evolution of surface morphology [13, 14] is responsible, at least in part, for this process. The smaller grain size and higher density of lattice defects accompanied by a higher hardness of the near-substrate region, caused a faster recrystallization at 500 °C and a lower hardness after subsequent cooling, as observed in Fig. 2.

The experiments with pure iron and steel substrates show that carbon present in the substrate plays a key role in the diffusion annealing of Fe–Ni alloy coatings (Fig. 3). According to the phase diagram (Fig. 1), during diffusion annealing below the α–γ transformation of the steel substrate (727 °C) the coating already contains a significant amount of γ-phase (solid solution of nickel in γ Fe, f c c). By taking advantage of this finding, diffusion annealing can be carried out in co-existence with α(substrate)–γ(coating) or γ(substrate)–γ(coating) diffusion couples.

Short-term annealing below 727 °C was not able to transport large amounts of carbon for long distances within the coating. For example, after 0.5 h at 710 °C the root mean square displacement for carbon diffusion in austenite is 31.6 μm ($D_C^{\gamma} = 5.5 \times 10^{-13}\,m^2s^{-1}$ at 710 °C, the influence of carbon and nickel content on diffusion are neglected [15]) which is in reasonable agreement with the hardness profile (Fig. 2). At the same time, the root mean square displacement for carbon in ferrite is 350 μm ($D_C^{\alpha} = 6.8 \times 10^{-11}\,m^2s^{-1}$ at 710 °C [15]) which means that carbon is easily supplied to the substrate–coating interface. The hardness of 486 HV, obtained after 0.5 h annealing at 710 °C, is the highest for all the temperatures of diffusion annealing examined. It is interesting to note that the substrate during annealing, remained pearlitic. Thus, at a high temperature, cementite coagulates, dissolves and acts as a source of carbon diffusing subsequently towards the coating. As a result, a thin layer of pure ferrite is formed at the substrate–coating interface (Figs 4b and 6a). According to the literature [16], such a thin ferritic layer can arrest the microcracks which nucleate during exploitation of the coating and prevent their propagation to the coated element.

Annealing above 727 °C provides a high diffusion flux of carbon from the substrate to the coating. After 0.5 h at 1000 °C the root mean square displacement for carbon in austenite is 268 μm ($D_C^{\gamma} = 2.5 \times 10^{-11} m^2s^{-1}$ at 1000 °C [15]), which means that carbon can penetrate almost the whole coating thickness. The high enrichment of coating in carbon and the presence of 14% Ni cause of large amount of retained austenite, which affects the hardness shown in Figs 2, 3 and 7. The mixture of hard martensite with the austenitic matrix is a microstructure having good wear behaviour. By designing the optimum volume fractions of both phases, the appropriate hardness can also be accomplished, for example a hardness of above 650 HV in the middle part of coating after carburizing (Fig. 7).

Thermal treatment also affects the internal stress in the coating. As reported previously [4, 8], Fe–Ni coatings after deposition are under tensile stress, reaching a level of approximately 800 MPa in the near-substrate region and then decreasing to 300 MPa close to the outer surface. It is well known that tensile stress will enhance the nucleation of microcracks and will reduce the fatigue life of a coated part [6]. The process of annealing at first relieves tensile stress. The phase transformations (bainitic or martensitic) which take place during subsequent cooling lead generally to an increase in the coating volume and to the origin of compressive stress, beneficial for fatigue life. Moreover, a strong adhesion is usually obtained when alloy formation occurs as a result of diffusion between substrate and coating [6]. An observation of the substrate/coating interface (Fig. 6a, b) indicates that in addition to carbon diffusion to the substrate, there is also nickel diffusion to the coating. The diffusion range of nickel is seen as a thin film within the ferritic layer in Fig. 6a and as a brighter contrast at grain boundaries of the former austenite in Fig. 6b. Thus the distinct interface present after deposition is replaced by the diffusion region with the benefit of coating adhesion.

The purpose of this research was not to design the optimum technological parameters for Fe–Ni coating hardening, but to assess the general changes which accompany post-deposition thermal or thermochemical treatment. Using these results, the surface treatment for particular coating thickness, substrate carbon content and service conditions, may be designed. Because Fe–Ni electrolytic alloys are also used at high temperatures [17], this study will help to understand their microstructural changes.

5. Conclusions

The hardness and microstructure of Fe–Ni alloy coatings deposited on a steel substrate can be effectively modified by diffusion annealing and by utilizing the transport of carbon from the substrate to the coating. In the case of low-carbon substrates the coating hardening can be improved by carburizing or carbonitriding.

Annealing of Fe–Ni coatings at a coexistence of α(substrate)–γ(coating) diffusion couple, leads to the enrichment of the coating in carbon and the formation of the ferritic layer at the substrate–coating interface. The enrichment of the coating in carbon is much higher after annealing at a coexistence of γ(substrate)–γ(coating) diffusion couple. The latter treatment leads to long-range and gradual decarburization of the steel substrate.

It is believed that Fe–Ni coatings with the microstructure modified by the post-deposition treatment described, and accompanied by microstructural changes in the substrate, will exhibit superior properties for some applications, in terms of adhesion, wear resistance, corrosion resistance and fatigue life.

Acknowledgements

The experimental part was conducted at the University of Mining and Metallurgy, Cracow, Poland. The author thanks Dr A. Zielinska-Lipiec for assistance with the TEM observations.

References

1. F. CZERWINSKI, H. LI, F. MEGRET, J. A. SZPUNAR, A. CLARK and U. ERB, *Scripta Mater.* **37** (1997) p. 1967.
2. K. N. STRAFFORD, P. K. DATTA and J. S. GRAY, "Surface Engineering Practice, Process, Fundamentals and Applications in Corrosion and Wear" (Ellis Horwood, New York, 1990) p. 399.
3. M. P. MIELKOW, "Coatings for the Automotive Industry" (Publ. Transport, Moscow, 1971).
4. F. CZERWINSKI, *Thin Solid Films* **280** (1996) 199.
5. F. CZERWINSKI and Z. KEDZIERSKI, *J. Mater. Sci.* **32** (1997) 2957.
6. W. H. SAFRANEK, "The Properties of Electrodeposited Metals and Alloys" (Elsevier, Amsterdam, 1974).
7. A. D. ROMING and J. I. GOLDSTEIN, *Metall. Trans.* **11** (1980) 1151.
8. F. CZERWINSKI, *J. Electroch. Soc.* **143** (1996) 3327.
9. G. KRAUSS, "Physical Metallurgy and Heat Treatment of Steel", in "Metals Handbook Desk Edition" (ASM, Materials Park, 1985).
10. T. BELL, *Heat Treat. Metals* **2** (1975) p. 39.
11. H. D. MERCHANT and O. B. GIRIN, in "Electrochemical Synthesis and Modification of Materials', edited by P. Andricacos *et al.*, (MRS, Pittsburgh, PA, 1997) p. 433.
12. F. CZERWINSKI, A. ZIELINSKA-LIPIEC and J. A. SZPUNAR, in "Textures of Materials-ICOTOM-11", edited by Z. Liang *et al.* (International Academic Publishers, Beijing, 1996) p. 1132.
13. K. KONDO, T. MURAKAMI, F. CZERWINSKI and K. SHINOHARA, *ISIJ Int.* **37** (1997) 140.
14. F. CZERWINSKI, K. KONDO and J. A. SZPUNAR, in "Electrochemical Synthesis and Modification of Materials", edited by P. Andricacos *et al.*, (MRS, Pittsburgh, PA, 1997) p. 445.
15. P. SHEWMON, "Diffusion in Solids" (TMS, Warrendale, PA, 1989).
16. R. W. HERTZBERG, "Deformation and Fracture Mechanics of Engineering Materials" (Wiley, New York, 1976).
17. H. KANAYAMA and A. ICHIHARA, *Kawasaki Steel Tech. Rep.* **7** (1983) 9.

Received 16 October 1997
and accepted 15 May 1998